Taylor & Francis
Taylor & Francis Group

Journal of Macromolecular Science, Part A
Pure and Applied Chemistry

ISSN: 1060-1325 (Print) 1520-5738 (Online) Journal homepage: https://www.tandfonline.com/loi/lmsa20

Characterization of poly(methyl methacrylate) nanofiber mats by electrospinning process

Ozcan Koysuren & H. Nagehan Koysuren

To cite this article: Ozcan Koysuren & H. Nagehan Koysuren (2016) Characterization of poly(methyl methacrylate) nanofiber mats by electrospinning process, Journal of Macromolecular Science, Part A, 53:11, 691-698, DOI: 10.1080/10601325.2016.1224627

To link to this article: https://doi.org/10.1080/10601325.2016.1224627

JOURNAL OF MACROMOLECULAR SCIENCE, PART A: PURE AND APPLIED CHEMISTRY
2016, VOL. 53, NO. 11, 691–698
http://dx.doi.org/10.1080/10601325.2016.1224627

Taylor & Francis
Taylor & Francis Group

Characterization of poly(methyl methacrylate) nanofiber mats by electrospinning process

Ozcan Koysuren[a] and H. Nagehan Koysuren[b]

[a]Department of Energy and Materials Engineering, Ankara University, Ankara, Turkey; [b]Department of Environmental Engineering, Ahi Evran University, Kirsehir, Turkey

ABSTRACT

In this study, the aim is to describe the influence of electrospinning parameters on the morphology, the water wetting property and dye adsorption property of poly(methyl methacrylate) nanofiber mats. Specifically, the effects of solution concentration, solvent type, applied voltage, distance between the electrodes and particulate reinforcement on the diameter and shape of the nanofibers were investigated. All poly(methyl methacrylate) nanofiber mats contained beaded nanofiber structures. With increasing the polymer solution concentration, the average fiber diameter also increased. Poly(methyl methacrylate) nanofiber mat electrospun from dimethylformamide solution resulted in thicker fibers when compared with the mat electrospun from acetone solution. Increasing the electric potential difference between the collector and the syringe tip did not increase the average fiber diameter. Besides increasing the distance between the electrodes resulted in a decrease in the average fiber diameter. When compared with PMMA nanofiber mat, thicker fibers were obtained with silica nanoparticles reinforced nanofiber mat. According to the water contact angle measurements, all poly(methyl methacrylate) nanofiber mats revealed hydrophobic surface property. PMMA nanofiber mat with the highest water contact angle gave rise to the highest dye adsorption capacity.

ARTICLE HISTORY
Received June 2016,
Revised and Accepted
July 2016

KEYWORDS
Nanofiber; electrospinning; process parameters; water contact angle; dye adsorption

1. Introduction

Materials, processed by controlling, assembling, manipulating and characterizing matter at atomic and molecular length-scale, are known as nanomaterials. Among one-dimensional nanostructures, nanowires, nanotubes, nanocylinders, nanotubules, nanorods and nanoribbons, nanofibers are the only one, describing properly mechanically flexible nanostructures of extremely high length-to-radius ratio (1). Polymer nanofibers with diameters in the range from several micrometers down to tens of nanometers are of considerable interest for various kinds of applications, including dye adsorbents, catalyst supports, drug delivery systems, fuel cells, conducting polymers and composites, photonics, sensors, medicine, pharmacy, wound dressings, filtration, tissue engineering, fiber mats serving as reinforcing component in composite systems and fiber templates for the preparation of functional nanotubes. Polymer in nanofiber form possesses an exceptionally high specific surface area, which results in quantum efficiency, nanoscale effect of unusually high surface energy, surface reactivity, high thermal and electrical conductivity, optical anisotropy, controllable porosity at nanoscale and high strength (1, 2).

Polymer nanofibers can be prepared by several methods such as drawing, template synthesis, phase separation, self-assembly and electrospinning. To produce nanomaterials using the cheapest and the most straightforward way, electrospinning is a novel process that produces superfine nanofibers by applying a high voltage charge to a polymer solution or melt and using the charge to draw the solution from the tip of a capillary to a grounded collector. This process system is basically composed of a syringe to hold the polymer solution, two electrodes and a DC voltage supply in the kV range, sufficient to overcome the surface tension forces of the polymer. The free surface of the charged polymer produces very fine jets of liquid, drawing to the grounded collector. The effect causes substantial drawing of the rapidly solidifying fibers as they approach the grounded collector. The fiber is collected as a web of fibers on the surface of the grounded collector (2–4).

Hydrophobic surfaces have attracted much interest in engineering due to their unique surface properties, including self-cleaning, anti-icing, and anti-sticking, that can find applications in photovoltaic, electronic and optical devices. Both surface energy and surface morphology are known to largely determine the final surface properties such as the water wetting property or hydrophobicity (5, 6). Only low surface energy is insufficient to achieve enhanced surface hydrophobicity. Rather, a combination of the surface energy and topography gives rise to the water-repellent properties (6–8). The hydrophobicity of a surface can be improved by being textured with different length scales of roughness. Herein, electrospinning process takes advantage of this by using a hierarchy of nano and microstructures on nanofiber coated surfaces to provide sufficient roughness for hydrophobicity (9).

Numerous studies have been reported that the processing parameters such as solution properties, the voltage supplied,

CONTACT Ozcan Koysuren koysuren@ankara.edu.tr Department of Energy and Materials Engineering, Ankara University, Ankara, 06830, Turkey.

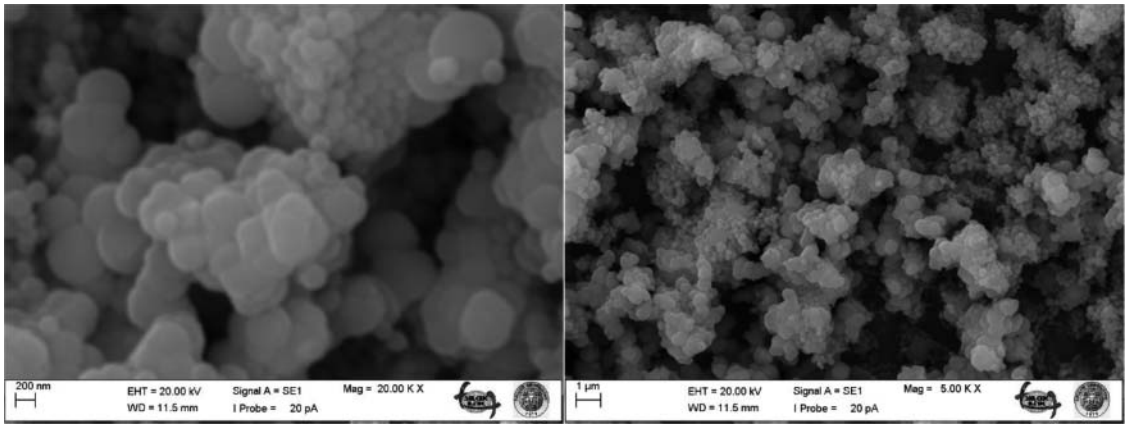

Figure 1. SEM micrographs of silica nanoparticles.

the feed rate, temperature of the solution, type of collector, diameter of needle and the distance between the needle tip and the collector affect the morphology of electrospun fibers. (3, 10–12). Hence, it is really important to investigate the processing conditions of electrospinning process. In addition, a growing research effort has been focused on dye adsorption property of electrospun mats. Studies on dye adsorption showed that the very large surface area and the high porosity confer high adsorption performances to electrospun mats (13–15). In this study, the effects of solution concentration, solvent type, applied voltage, distance between the electrodes and particulate reinforcement on the fiber morphology, the water wetting property and dye adsorption property of electrospun poly(methyl methacrylate) (PMMA) mats were studied.

2. Experimental

Poly(methyl methacrylate) (product # AB211664) was purchased from ABCR, Germany. PMMA was dissolved in acetone to obtain 2, 4 and 6 wt% solutions. For comparison purpose, PMMA was also dissolved in dimethylformamide (DMF) to obtain 4 wt% solution. Laboratory scale electrospinning unit (NE-100, Inovenso) was used to prepare PMMA nanofiber mats. The solutions, fed into a syringe, were delivered using a syringe pump to maintain a steady flow of 0.1 ml/hr. An electric potential difference of 20 kV was applied between the collector and the syringe tip. For comparison purpose, 30 kV and 40 kV electric potential differences were also applied to 4 wt% PMMA-acetone solution. The distance between the collector and the tip was 10 cm. As a process parameter, the distance between the electrodes was changed to 19 cm during the electrospinning of 6 wt% PMMA-acetone solution. Silica nanoparticles (Figure 1), prepared according to the classical Stöber method in the laboratory before (16), was used and mixed with 2 wt% PMMA-acetone solution to obtain 16 wt% silica/PMMA composite solution. An electric potential difference of 40 kV was applied between the electrodes to prepare silica nanoparticles reinforced nanofiber mat. Electrospun PMMA nanofibers were collected on aluminum foil. PMMA nanofiber mats with their codes and processing conditions are summarized in Table 1. To investigate the effect of nanofiber morphology on the water wetting property, PMMA film was prepared using a Laurell Model (WS-400BZ-6NP/LITE) spin-coater at 2000 rpm.

The microstructure and surface morphologies of the PMMA nanofiber mats were observed by a scanning electron microscope (SEM: EVO LS10 ZEISS). The average fiber diameter and its standard deviation were determined using an image analysis software (National Institutes of Health Images) from the SEM images of the PMMA nanofiber mats. At least 20 different fibers were analyzed for this purpose. The water contact angles of the PMMA nanofiber mats and the spin coated PMMA film were obtained using the sessile drop method with a drop shape analysis system (Krüss, easydrop model) at room temperature. Three different contact angle measurements were performed for each system and average of these three test results were given with their standard deviations. Dye adsorption tests were conducted by immersing PMMA nanofiber mat sample of 3×3 cm^2 into 50 ml methylene blue solution with a concentration of 10 mg/L. The dye concentration was determined with a UV–visible spectrophotometer (UV-Mini 1240 Spectrophotometer) at 665 nm. The adsorption capacity q (mg/g) was calculated using the following equation:

$$q = \frac{(c_o - c_e)V}{m}$$

where c_o (mg/L)and c_e (mg/L) are the initial and the equilibrium methylene blue concentrations, respectively. V (L) is the

Table 1. The PMMA nanofiber mats with their codes and electrospinning conditions.

Codes	PMMA composition of solution	Solvent type	Electric potential difference between the collector and the syringe tip	The distance between the collector and the syringe tip	Particulate reinforcement
PMMA1	2 wt. %	acetone	20 kV	10 cm	—
PMMA2	4 wt. %	acetone	20 kV	10 cm	—
PMMA3	6 wt. %	acetone	20 kV	10 cm	—
PMMA4	2 wt. %	acetone	40 kV	10 cm	—
PMMA5	2 wt. %	acetone	40 kV	10 cm	silica
PMMA6	4 wt. %	DMF	20 kV	10 cm	—
PMMA7	4 wt. %	acetone	30 kV	10 cm	—
PMMA8	4 wt. %	acetone	40 kV	10 cm	—
PMMA9	6 wt. %	acetone	20 kV	19 cm	—

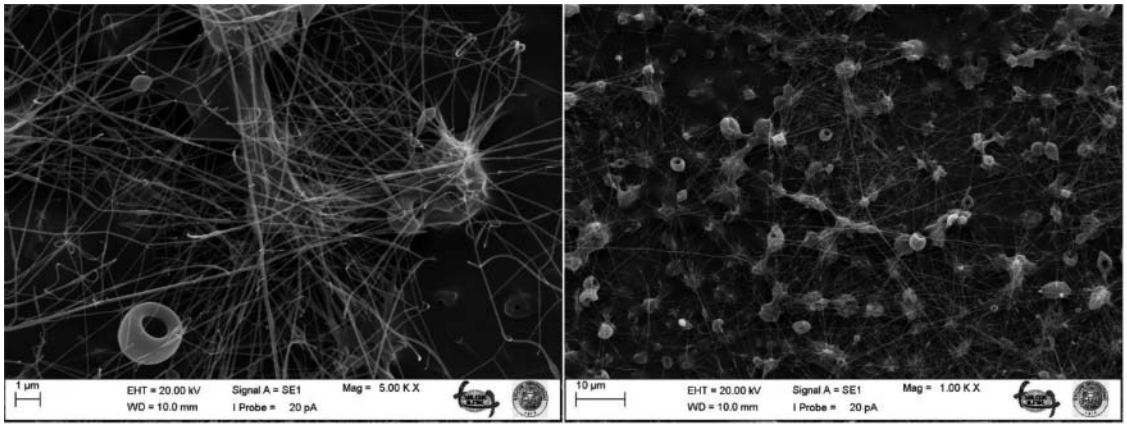

Figure 2. SEM micrographs of PMMA1 mat.

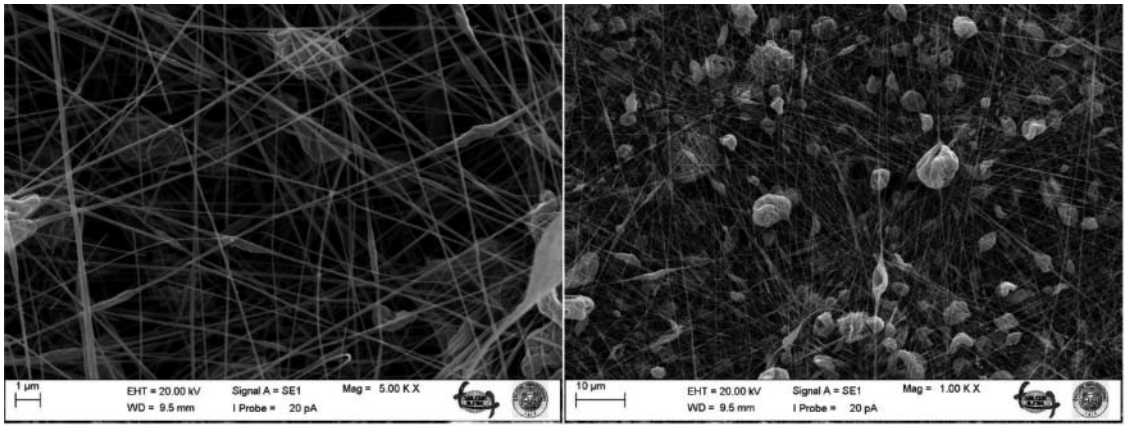

Figure 3. SEM micrographs of PMMA2 mat.

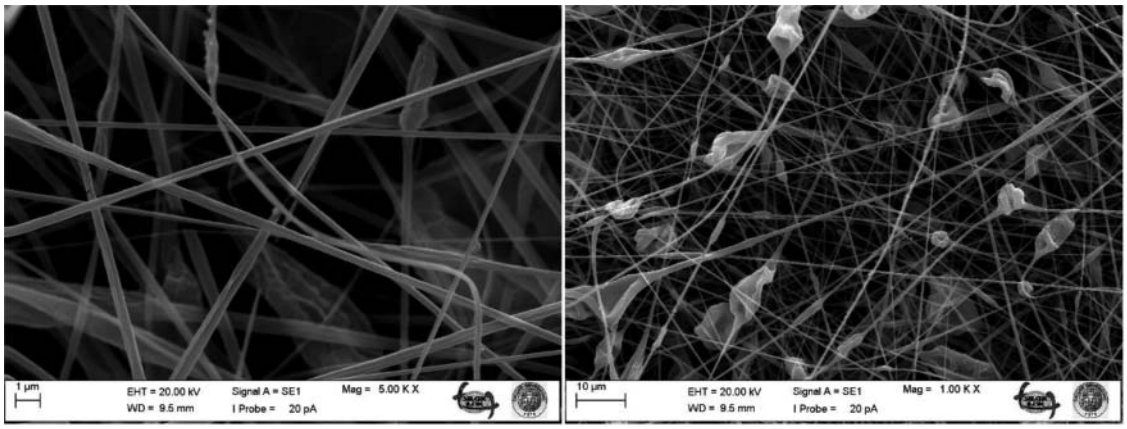

Figure 4. SEM micrographs of PMMA3 mat.

volume of the solution and m (g) is the weight of the mat sample.

3. Results and discussion

The viscosity of the polymer solution plays a significant role in the electrospinning process and the resultant fiber morphology (3, 17). The viscosity of the polymer solution is mainly affected by two different parameters, which are solvent type and polymer concentration. The polymer solution concentration has a significant effect on the final size and the shape of the electrospun particle (3, 18). An increase in the polymer solution concentration gives rise to an increase in the solution viscosity. Moreover, addition of silica nanoparticles into PMMA solution might result in an increase in the solution viscosity. With increased solution viscosity, the diameter of the electrospun fiber also increases (3, 7, 17). SEM images of PMMA1, PMMA2 and PMMA3 illustrate that increasing the polymer

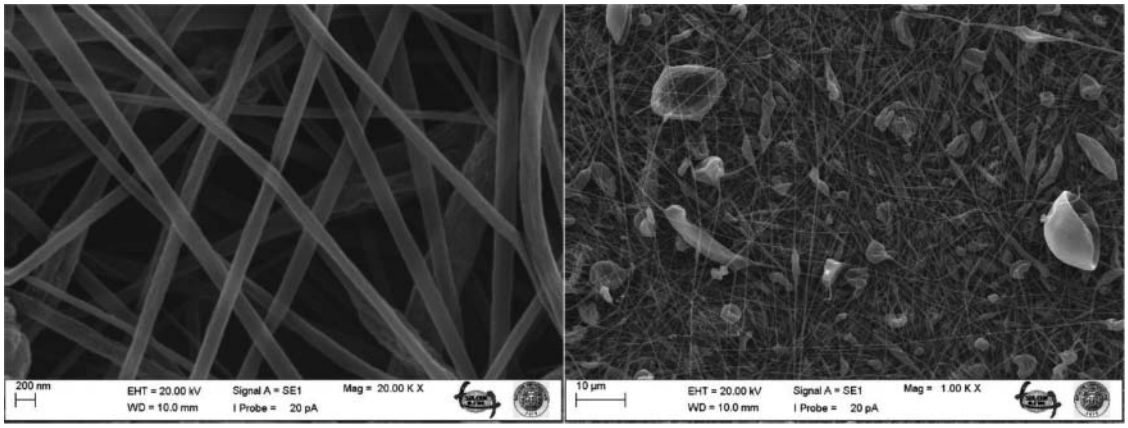

Figure 5. SEM micrographs of PMMA4 mat.

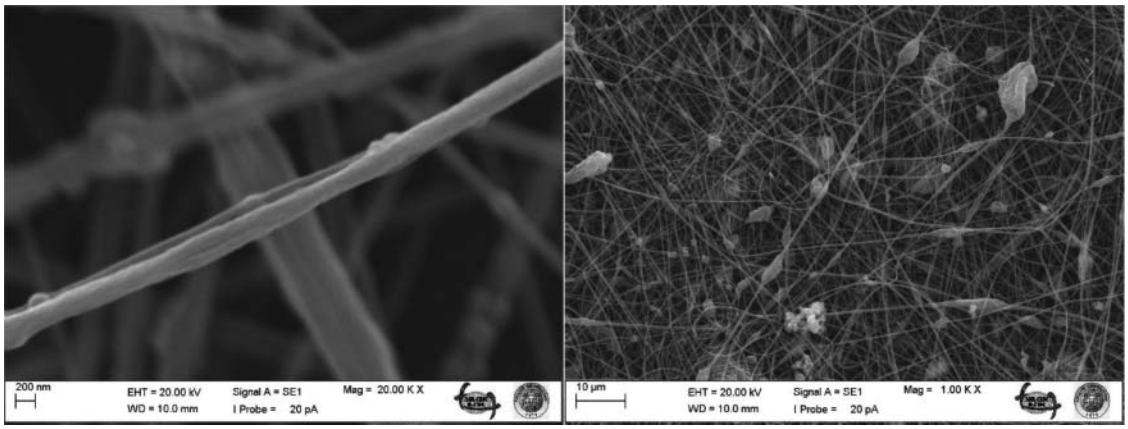

Figure 6. SEM micrographs of PMMA5 mat.

solution concentration from 2 to 6 wt% increased the average fiber diameter (Figures 2–4). According to SEM images, PMMA4 solution yielded beaded fiber structures with an average fiber diameter of 194 nm and silica nanoparticles reinforced PMMA solution yielded beaded fiber structures with an average fiber diameter of 307 nm (Figures 5 and 6).

When different solvents are used to make polymer solutions with the same concentration, polymer solutions with different viscosities can be obtained (19). A solution with a relatively high viscosity gives rise to an increase in the diameter of the electrospun fibers (3, 17). According to Table 2, the average fiber of PMMA6 mat is thicker than the average fiber diameter of PMMA2 mat (Figures 3 and 7), which should be the result of different viscosities of polymer solutions made by different solvents at the same concentration (19). For electrospinning, if the polymer solution viscosity is low owing to the low solution concentration, the electrospinning process generates beaded fibers instead of smooth fibers (3, 7, 18). This is the reason for the beaded fibers observed on the SEM images of the PMMA nanofiber mats (Figures 2–10). A minimum viscosity for each polymer solution is required to yield fibers without beads (3, 17).

Table 2. The average diameter of PMMA nanofibers with their standard deviations and the water contact angle of the electrospun PMMA mats with their standard deviations.

Sample	Average diameter (nm)	Water contact angle
PMMA1	101 ± 38	124.6° ± 2.3°
PMMA2	160 ± 63	129.3° ± 6.1°
PMMA3	341 ± 54	134.6° ± 3.0°
PMMA4	194 ± 48	130.3° ± 4.3°
PMMA5	307 ± 61	147.1° ± 10.3°
PMMA6	517 ± 66	123.2° ± 4.1°
PMMA7	1419 ± 138	132.2° ± 2.0°
PMMA8	762 ± 92	135.6° ± 2.6°
PMMA9	263 ± 98	100.1° ± 5.4°

Another important parameter that affects the electrospinning process is the electric potential difference between the collector and the syringe tip. If the electric potential difference is higher, the greater amount of charges will cause the jet to accelerate faster and more volume of solution will be drawn from the tip of the needle. As the electric potential difference between the electrodes has an influence in the stretching and the acceleration of the jet, it will have an influence on the morphology of the fibers obtained. In most cases, a higher potential difference will have the effect of reducing the diameter of the fibers (3). However, this trend could not been seen among PMMA2, PMMA7 and PMMA8. PMMA2 mat possesses the thinnest fiber diameter among those electrospun mats (Figures 3, 8 and 9, Table 2).

As a process parameter, varying the distance between the tip and the collector will have a direct influence in the flight time, which will affect the electrospinning process and the resultant fibers. When the distance between the tip and the collector is increased, the jet will have a longer distance to travel before it

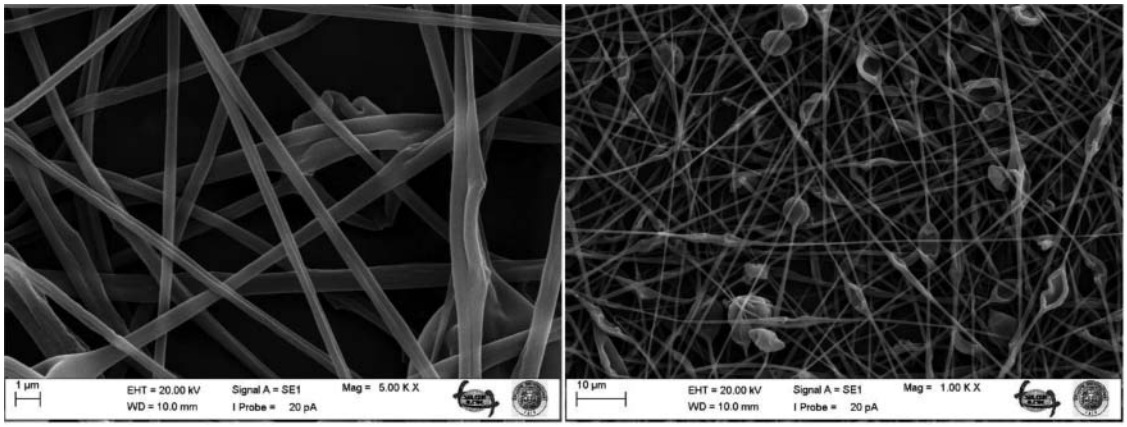

Figure 7. SEM micrographs of PMMA6 mat.

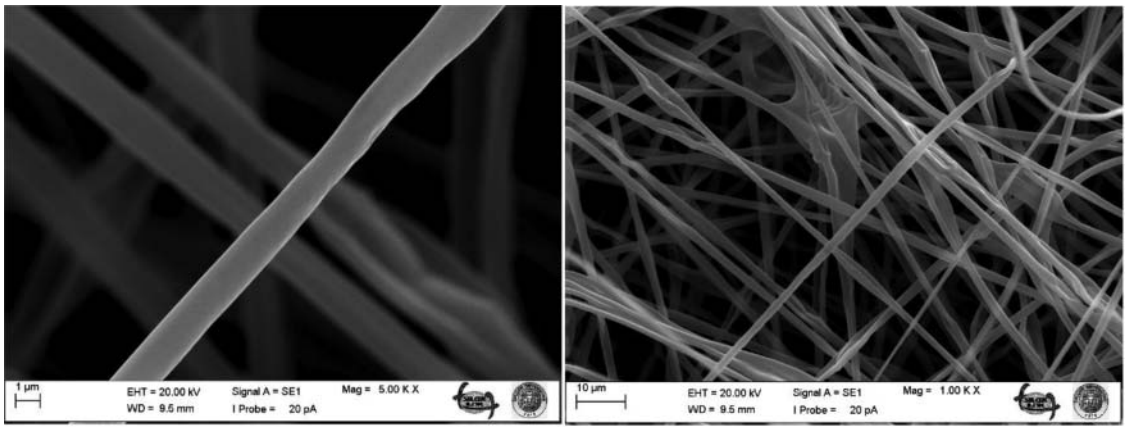

Figure 8. SEM micrographs of PMMA7 mat.

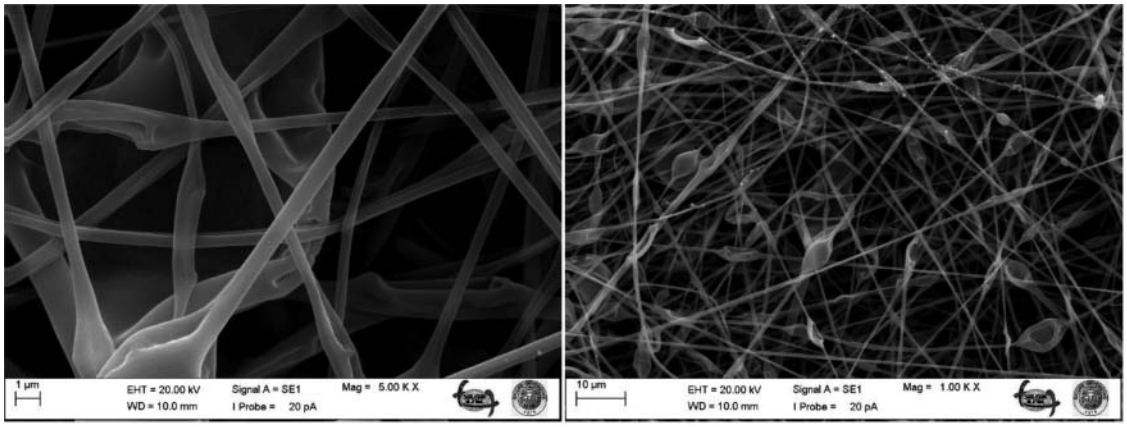

Figure 9. SEM micrographs of PMMA8 mat.

reaches the collector plate. The longer distance means that there is a longer flight time for the solution to be stretched before it is deposited on the collector. Hence, increasing the distance between the tip and the collector results in a decrease in the average fiber diameter (3). As expected, PMMA9 mat possesses thinner fiber diameter when compared with PMMA3 mat (Figures 4 and 10). Increasing the distance between the electrodes from 10 cm to 19 cm gave rise to a decrease in the average fiber diameter from 341 nm to 263 nm (Table 2).

Hydrophilic surfaces show a contact angle between 0° and 30°. Moreover, less hydrophilic surfaces exhibit a contact angle up to 90°. Materials with a contact angle more than 90° is termed as hydrophobic (20). The images and the results of water contact angle measurements are shown in Figure 11 and in Table 2, respectively. Figure 11a illustrates a water droplet formed on the spin coated PMMA film. The surface contact angle of the spin coated film is 76.6°, which was measured as a reference to the electrospun PMMA mats. Hence, the spin coated film revealed less hydrophilic surface property. The images of the electrospun mats illustrate a significant increase in the contact angle, which may be ascribed to the enhanced surface roughness (Figure 11, Table 2). The surface roughness

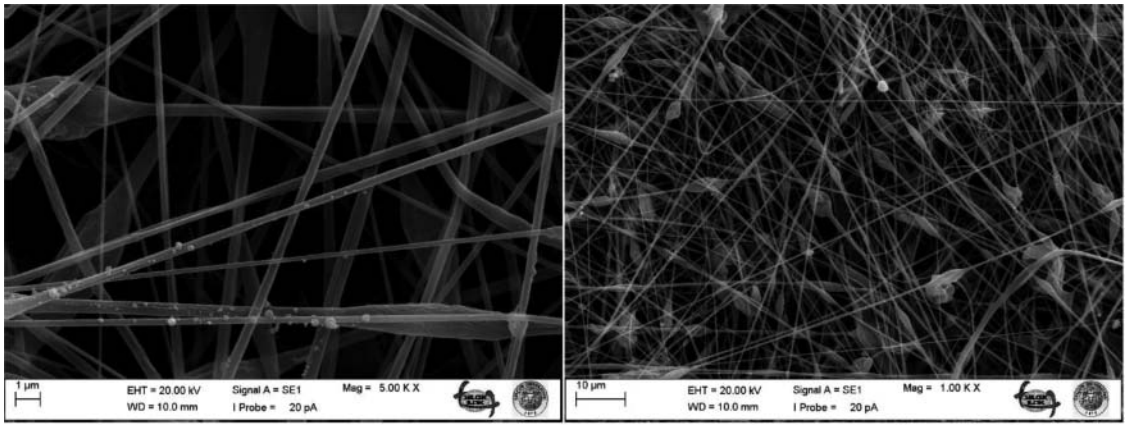

Figure 10. SEM micrographs of PMMA9 mat.

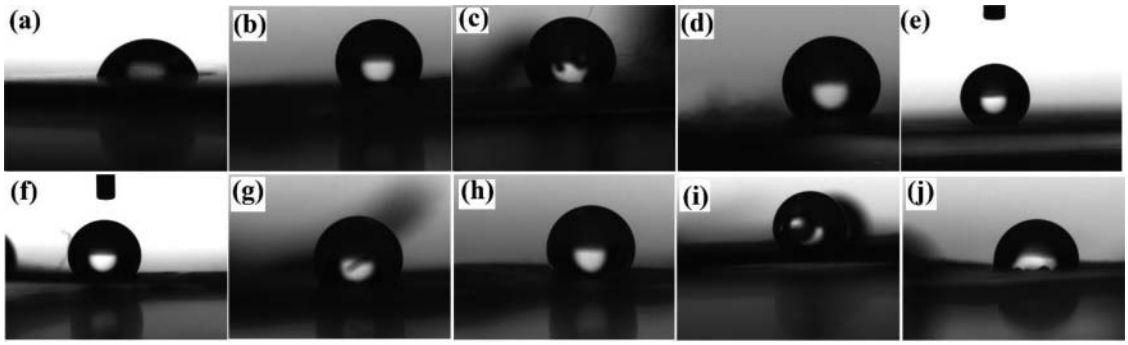

Figure 11. Water contact angle images of (a) the spin coated PMMA film, (b) PMMA1 mat, (c) PMMA2 mat, (d) PMMA3 mat, (e) PMMA4 mat, (f) PMMA5 mat, (g) PMMA6 mat (h) PMMA7 mat, (i) PMMA8 mat and (j) PMMA9 mat.

and the porosity have significant effect on the apparent contact angle (18, 21–23). In addition, all the electrospun mats revealed hydrophobic surface property.

With an increase in fiber diameter, the surface roughness of the electrospun mat can increase (24, 25). As expected, increasing the polymer solution concentration from 2 to 6 wt% increased both the average fiber diameter and the water contact angle (Table 2, Figure 11). However, this trend could not be seen among other electrospun mats (Table 2). There should be an optimum fiber diameter for enhanced surface roughness and hydrophobicity. The surface roughness and the porosity of the electrospun mat can also be enhanced by modifying the fiber dimension with bead structures (7, 21, 22). Although all the electrospun PMMA mats show beaded fiber structures (Figures 2–10), the highest water contact angle of 147.1° was obtained with PMMA5 mat. More enhanced surface roughness might be obtained with silica nanoparticles reinforced nanofiber mat.

Figure 12 illustrates the results of methylene blue adsorption tests. In the first 30 minutes, a rapid adsorption was observed, which might be due to the presence of adsorption sites, and then the removal was almost constant (13). The adsorption capacity values of PMMA1, PMMA3, PMMA5, PMMA8 and PMMA9 mats were 5.6, 5.3, 6.5, 5.4 and 5.1 mg/g, respectively. When compared with PMMA1, PMMA3, PMMA8 and PMMA9 mats, the stronger adsorption capacity of PMMA5 mat might be due to the enhanced surface roughness and hydrophobicity obtained with silica nanoparticles introduction, leading methylene blue molecules to adhere on the mat surface easily (14). In addition, the pseudo-first order and pseudo-second order models were used to study the adsorption kinetic character of PMMA nanofiber mats. The pseudo-first order and pseudo-second order models are given below (13, 14):

$$\log(q_e - q_i) = \log q_e - k_1 t$$

$$\frac{t}{q_i} = \frac{1}{k_2 q_e^2} + \frac{t}{q_e}$$

where q_i (mg/g)and q_e (mg/g) are the adsorption capacity at time t and at equilibrium, respectively. k_1 (min^{-1}) and k_2 (g/mg.min) are the adsorption rate constants of the pseudo-first order and pseudo-second order models, respectively.

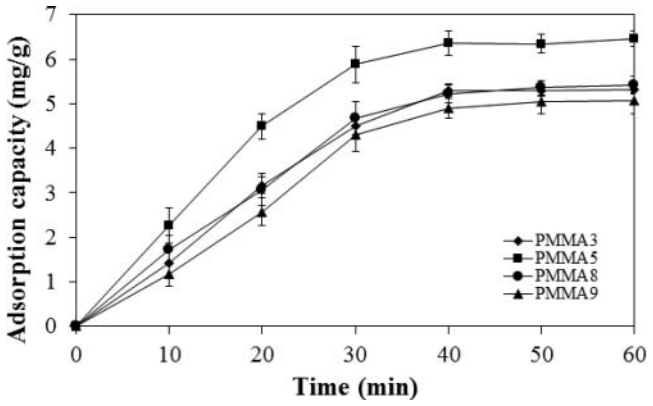

Figure 12. The adsorption capacity of PMMA nanofiber mats for methylene blue.

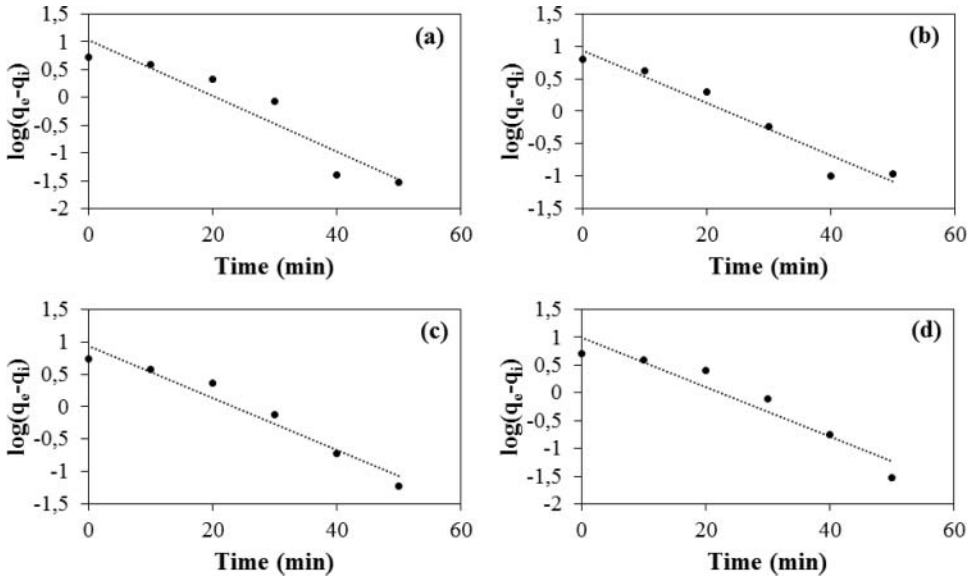

Figure 13. The plots of the pseudo-first order model for methylene blue adsorption by (a) PMMA3 mat, (b) PMMA5 mat, (c) PMMA8 mat and (d) PMMA9 mat.

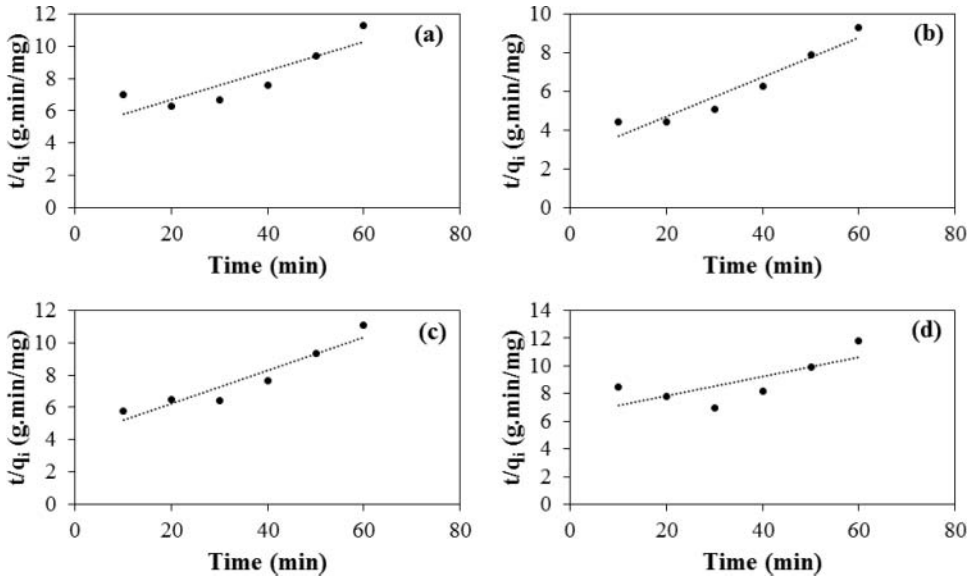

Figure 14. The plots of the pseudo-second order model for methylene blue adsorption by (a) PMMA3 mat, (b) PMMA5 mat, (c) PMMA8 mat and (d) PMMA9 mat.

The plots of $log(q_e\text{-}q_i)$ vs. t (Figure 13) and t/q_i vs. t (Figure 14) were used to determine the model parameters for methylene blue adsorption on PMMA nanofiber mats (Table 3). When comparing the correlation coefficient (R^2) values, the adsorption process was better described by the pseudo-first order model (Table 3).

Table 3. The model parameters for methylene blue adsorption on the PMMA nanofiber mats.

	Pseudo-first order			Pseudo-second order		
Adsorbent	q_e (mg/g)	k_1	R^2	q_e (mg/g)	k_2	R^2
PMMA3	10.84	0.0504	0.8934	11.09	0.0017	0.7716
PMMA5	8.69	0.0407	0.9442	9.76	0.0039	0.9272
PMMA8	8.78	0.0404	0.9519	9.69	0.0025	0.9011
PMMA9	10.09	0.0447	0.9180	14.35	0.0008	0.5585

4. Conclusions

Electrospinning process parameters have shown implications on the morphology, the water wetting property and dye adsorption property of the PMMA nanofiber mat. SEM images and water contact angle measurements indicate that electrospinning parameters like solution concentration, solvent type, applied voltage, distance between the electrodes and particulate reinforcement had significant impact on the average fiber diameter and the surface hydrophobicity. The thinnest fiber structure was observed on PMMA1 mat. The highest water contact angle and the strongest adsorption capacity were obtained with PMMA5 mat. This study has shown that understanding of the electrospinning process parameters can lead to the possibility of controlling the morphology, the water wetting property and dye adsorption property of nanofiber mats.

Acknowledgements

The authors thank Canan Duran and Irem Arslan, undergraduate students from the Department of Chemical Engineering of Selcuk University for their support for running certain experiments.

References

1. Pisignano, D. Polymer Nanofibers: Building Blocks for Nanotechnology, RSC Publishing: Cambridge, UK, Chapter 1, 2013.
2. He, J. H., Liu, Y., Mo, L. F., Wan, Y. Q., Xu, L. Electrospun Nanofibres and Their Applications, iSmithers: Shropshire, UK, 2008.
3. Ramakrishna, A., Fujihara, K., Teo, W. E., Lim, T. C., Ma, Z. An Introduction to Electrospinning and Nanofibers, World Scientific Publishing: London, 2005.
4. Hutten, I. M. Handbook of Non-Woven Filter Media, Elsevier Science & Technology Books: Oxford, UK, 2007.
5. Li, Y., Cai, W., Duan, G., Cao, B., Sun, F., Lu, F. (2005) J. Colloid. Interf. Sci., 287, 634–639.
6. Norek, M., Krasinski, A. (2015) Surf. Coat. Tech., 276: 464–470.
7. Koysuren, O., Karaman, M., Yildiz, H. B., Koysuren, H. N., Dinc, H. (2014) Int. J. Polym. Mater., 63: 337–341.
8. Karaman, M., Çabuk, N., Özyurt, D., Köysüren, Ö. (2012) Appl. Surf. Sci., 259: 542–546.
9. Lin, F., Zhang, Y., Xi, J., Zhu, Y., Wang, N., Xia, F., Jiang, L. (2008) Langmuir, 24: 4114–4119.
10. Awal, A., Sain, M., Chowdhury, B. (2011) Compos. Part B, 42: 1220–1225.
11. Xia, X., Wang, X., Zhou, H., Niu, X., Xue, L., Zhang, X., Wei, Q. (2014) Electrochim. Acta, 121: 345–351.
12. Neo, Y. P., Ray, S., Easteal, A. J., Nikolaidis, M. G., Quek, S. Y. (2012) J. Food Eng., 109(4): 645–651.
13. Zhao, R., Wang, Y., Li, X., Sun, B., Jiang, Z., Wang, C. (2015) Colloid. Surface. B, 136: 375–382.
14. Guo, J., Zhang, Q., Cai, Z., Zhao, K. (2016) Sep. Purif. Technol., 161: 69–79.
15. Aluigi, A., Rombaldoni, F., Tonetti, C., Jannaoke, L. (2014) J. Hazard. Mater., 268: 156–165.
16. Stöber, W., Fink, A., Bohn, E. (1968) J. Colloid Interf. Sci., 26(1): 62–69.
17. Uslu, I., Tunc, T., Ozturk, M. K., Aytimur, A. (2012) Polym.-Plast. Technol., 51: 257–262.
18. Ding, B., Kim, H. Y., Lee, S. C., Lee, D. R., Choi, K. J. (2002) Fiber. Polym., 3: 73–79.
19. Kanani, A. G., Bahrami, S. H. (2011) J. Nanomater., 2011: 1–10.
20. Shalumon, K. T., Anulekha, K. H., Chennazhi, K. P., Tamura, H., Nair, S. V., Jayakumar, R. (2011) Int. J. Biol. Macromol., 48: 571–576.
21. Ma, M., Gupta, M., Zhi, L., Zhai, L., Gleason, K. K., Cohen, R. E. (2007) Adv. Mater., 19: 255–259.
22. Rawal, A. (2011) Mater. Lett., 65: 1457–1459.
23. Sarkar, M. K., Bal, K., He, F., Fan, J. (2011) Appl. Surf. Sci., 257: 7003–7009.
24. Zhijiang, C., Yi, X., Haizheng, Y., Jia, J., Liu, Y. (2016) Mat. Sci. Eng. C, 58: 757–767.
25. Singh, A., Steely, L., Allcock, H. R. (2005) Langmuir, 21: 11604–11607.